Supplementary material

Oleksii M Matsiaka[1], Ruth E Baker[2], *Matthew J Simpson[1]

[1] *School of Mathematical Sciences, Queensland University of Technology (QUT) Brisbane, Queensland, Australia.*

[2] *Mathematical Institute, University of Oxford, Radcliffe Observatory Quarter, Woodstock Road, Oxford, United Kingdom.*

Contents

* Corresponding author
Email address: matthew.simpson@qut.edu.au, *Telephone* + 617 3138 5241, *Fax* + 617 3138 2310 (*Matthew J Simpson[1]).

A Heterogeneity in the interaction force, f_0

In this data set we explore the heterogeneity in the interaction force, f_0. Here we fix values of diffusivity, $D = 250\,\mu\text{m}^2/\text{h}$, and cell size, $\delta = 34\,\mu\text{m}$. To analyse performance of the single-species homogeneous model (Equation (3.9), Main paper) applied to a data generated by the three-species heterogeneous model (Equations (3.2)-(3.4), Main paper) we consider four interaction force distributions: (i) uniform distribution, Figure A.1(a), (ii) monotonically decreasing distribution, Figure A.2(a), (iii) non-monotonic distribution, Figure A.3(a), and (iv) monotonically increasing distribution, Figure A.4(a). For all cases presented we are able to predict a position of the leading edge as well as accurately describe cell density profiles given by the three-species heterogeneous model.

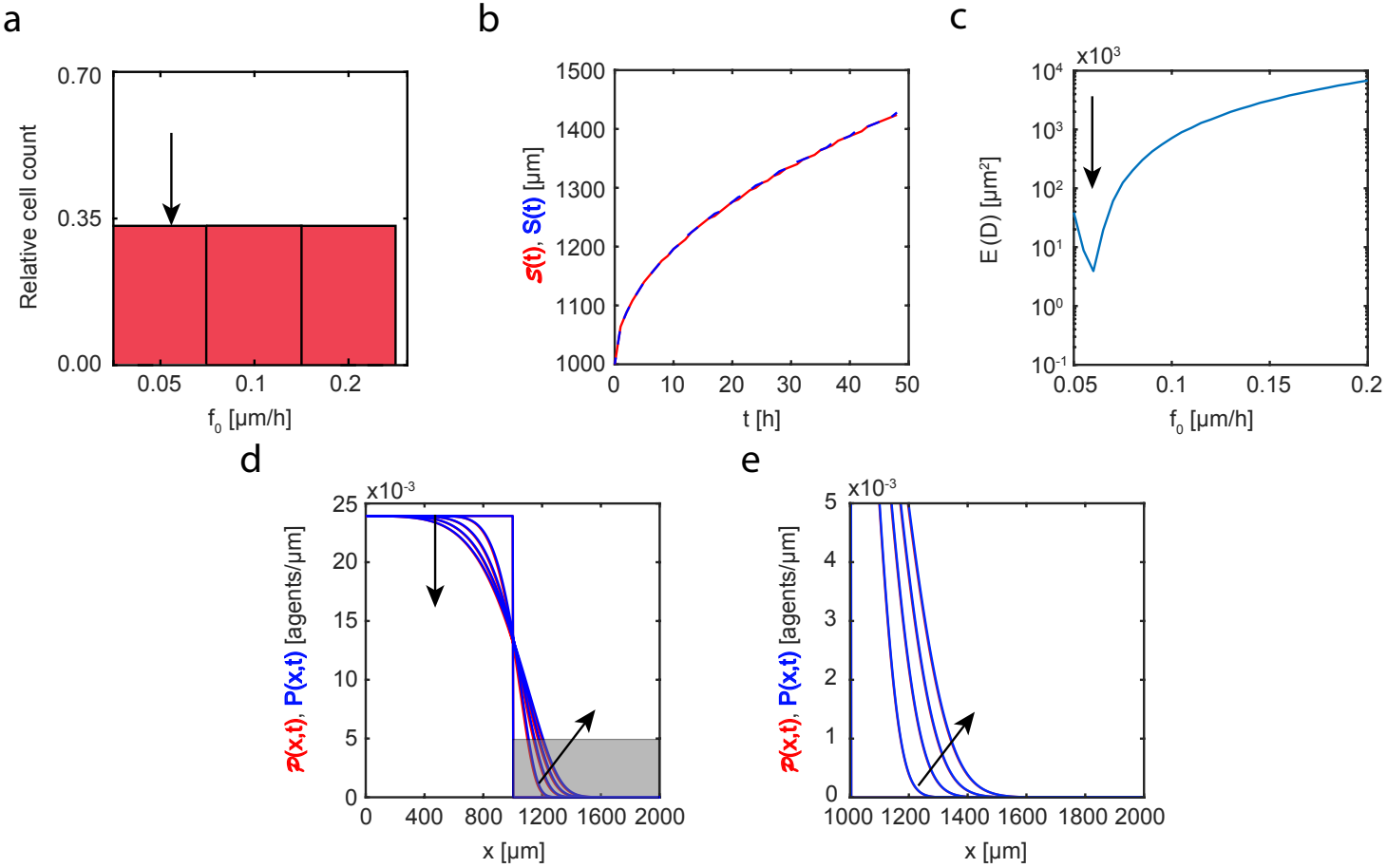

Fig. A.1. Set IIa. Heterogeneity in interaction forces: uniform distribution. (a): Interaction force distribution adopted in the three-species heterogeneous model, Equations (3.2)-(3.4) (Main paper). (b): Leading edge predicted by the three-species heterogeneous model, $\mathcal{S}(t)$ (solid red), and the best-fit approximation given by the single-species homogeneous model, $S(t)$ (blue dashed). (c): Error measure, $E(f_0)$, between the density profiles given by the three-species heterogeneous model and the profiles predicted by the single-species homogeneous model as a function of amplitude of the interaction force, f_0. (d)-(e): Cell density profiles predicted by the three-species heterogeneous model, $\mathcal{P}(x,t)$ (solid red), superimposed with density profiles given by the single-species homogeneous model calibrated with the best-fit value of f_0, $P(x,t)$ (solid blue). The black arrow denotes the best-fit value of interaction force, $f_0 = 0.055\,\mu$m/h. The continuum results for both models are presented at $t = 0, 12, 24, 36$, and 48 h. Black arrows denote the direction of increasing time. Results in (e) show a close-up comparison right near the leading edge, denoted by the gray shaded region in (d).

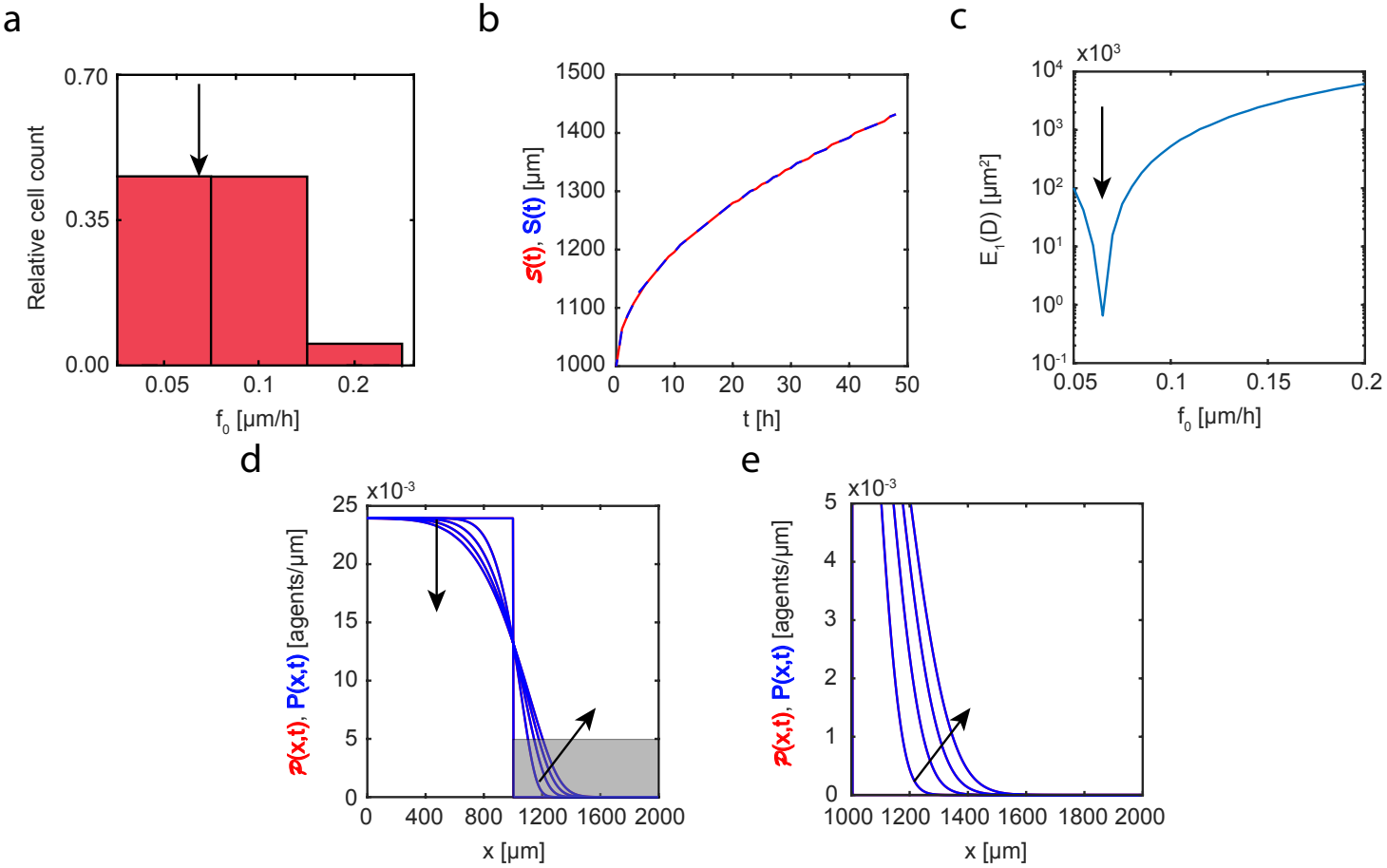

Fig. A.2. Set IIb. Heterogeneity in interaction forces: monotonically decreasing distribution. (a): Interaction force distribution adopted in the three-species heterogeneous model, Equations (3.2)-(3.4) (Main paper). (b): Leading edge predicted by the three-species heterogeneous model, $\mathcal{S}(t)$ (solid red), and the best-fit approximation given by the single-species homogeneous model, $S(t)$ (blue dashed). (c): Error measure, $E(f_0)$, between the density profiles given by the three-species heterogeneous model and the profiles predicted by the single-species homogeneous model as a function of amplitude of the interaction force, f_0. (d)-(e): Cell density profiles predicted by the three-species heterogeneous model, $\mathcal{P}(x,t)$ (solid red), superimposed with density profiles given by the single-species homogeneous model calibrated with the best-fit value of f_0, $P(x,t)$ (solid blue). The black arrow denotes the best-fit value of interaction force, $f_0 = 0.06\,\mu$m/h. The continuum results for both models are presented at $t = 0, 12, 24, 36$, and 48 h. Black arrows denote the direction of increasing time. Results in (e) show a close-up comparison right near the leading edge, denoted by the gray shaded region in (d).

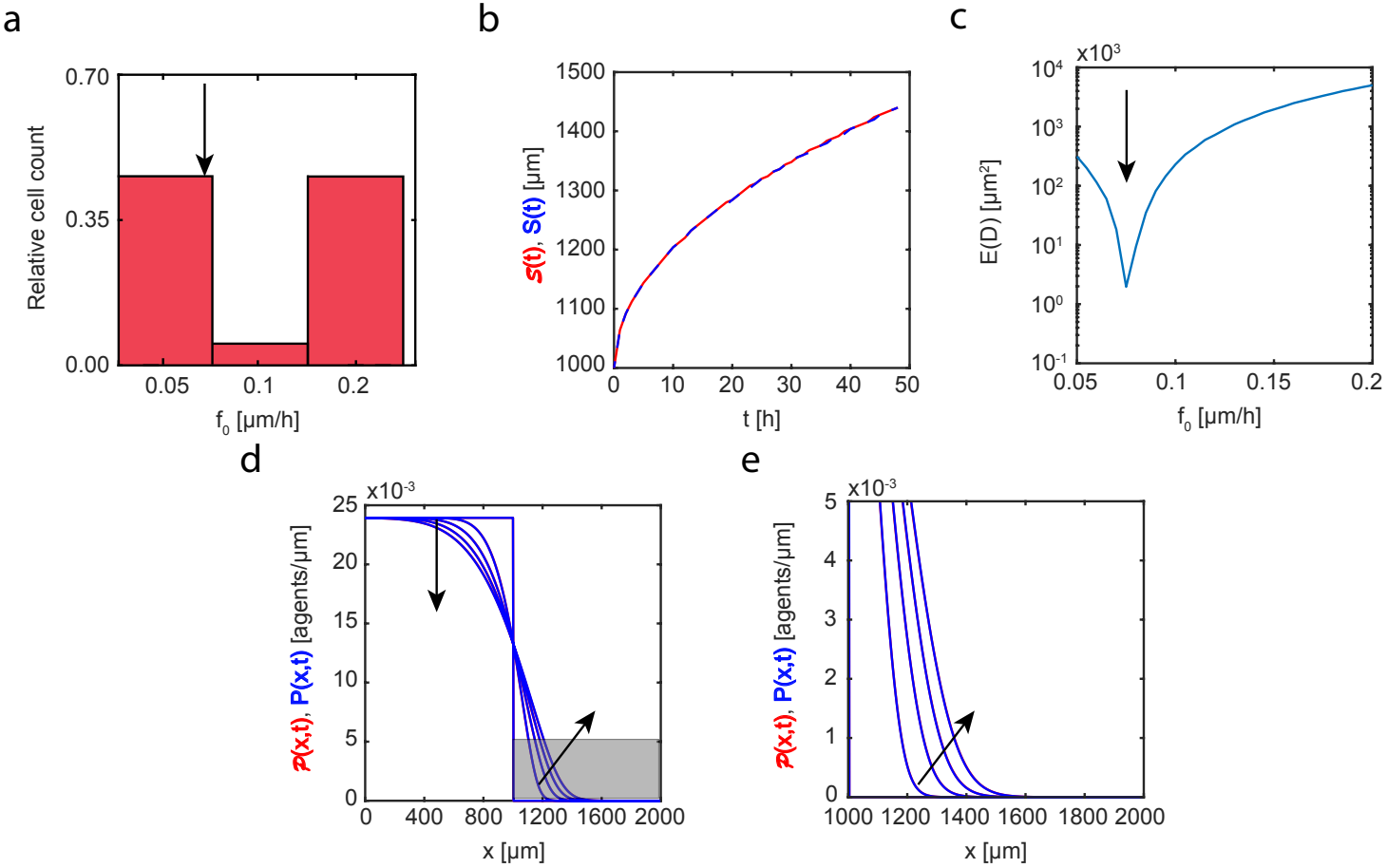

Fig. A.3. Set IIc. Heterogeneity in interaction forces: non-monotonic distribution. (a): Interaction force distribution adopted in the three-species heterogeneous model, Equations (3.2)-(3.4) (Main paper). (b): Leading edge predicted by the three-species heterogeneous model, $\mathcal{S}(t)$ (solid red), and the best-fit approximation given by the single-species homogeneous model, $S(t)$ (blue dashed). (c): Error measure, $E(f_0)$, between the density profiles given by the three-species heterogeneous model and the profiles predicted by the single-species homogeneous model as a function of amplitude of the interaction force, f_0. (d)-(e): Cell density profiles predicted by the three-species heterogeneous model, $\mathcal{P}(x,t)$ (solid red), superimposed with density profiles given by the single-species homogeneous model calibrated with the best-fit value of f_0, $P(x,t)$ (solid blue). The black arrow denotes the best-fit value of interaction force, $f_0 = 0.065\,\mu$m/h. The continuum results for both models are presented at $t = 0, 12, 24, 36$, and 48 h. Black arrows denote the direction of increasing time. Results in (e) show a close-up comparison right near the leading edge, denoted by the gray shaded region in (d).

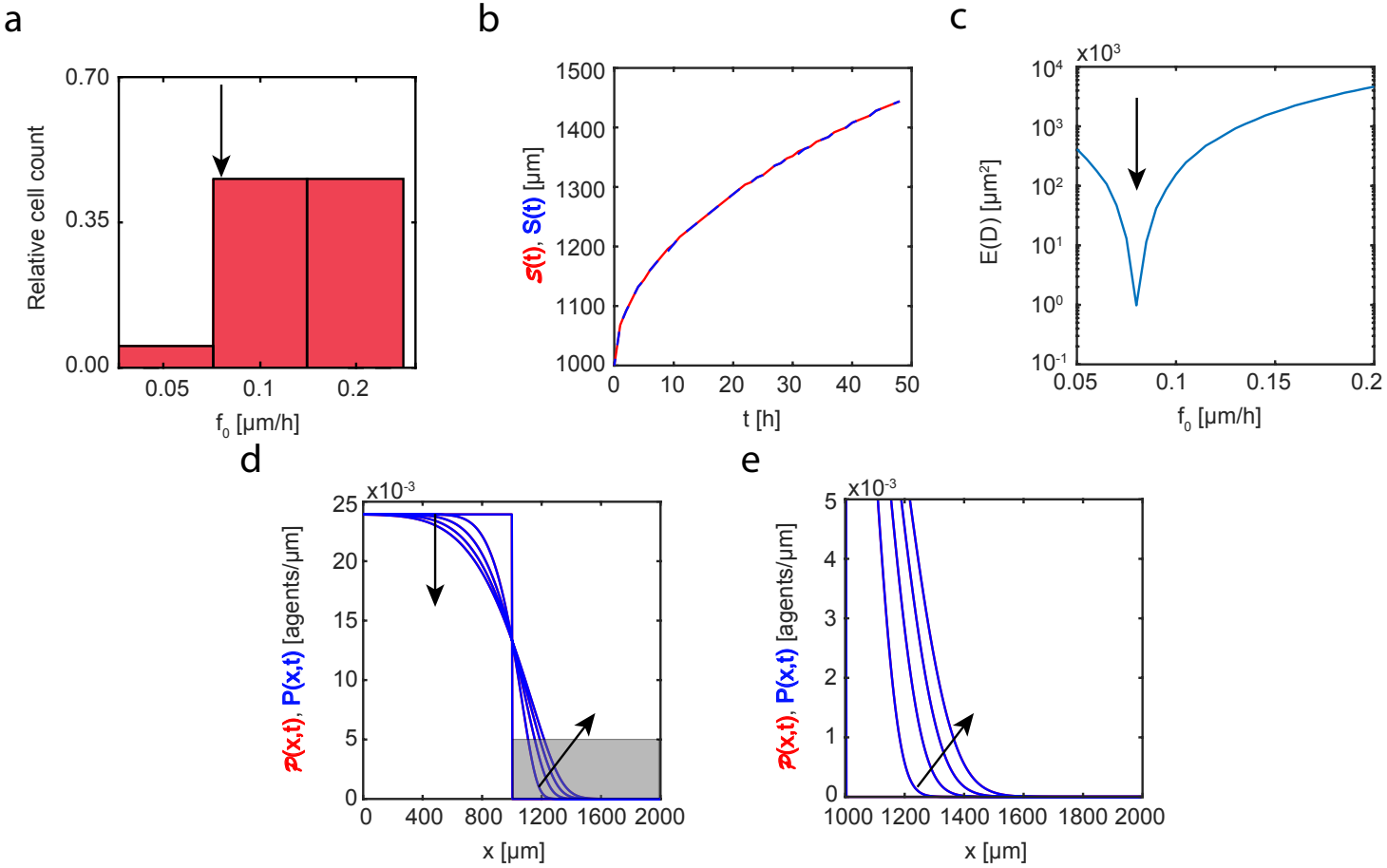

Fig. A.4. Set IId. Heterogeneity in interaction forces: monotonically increasing distribution. (a): Interaction force distribution adopted in the three-species heterogeneous model, Equations (3.2)-(3.4) (Main paper). (b): Leading edge predicted by the three-species heterogeneous model, $\mathcal{S}(t)$ (solid red), and the best-fit approximation given by the single-species homogeneous model, $S(t)$ (blue dashed). (c): Error measure, $E(f_0)$, between the density profiles given by the three-species heterogeneous model and the profiles predicted by the single-species homogeneous model as a function of amplitude of the interaction force, f_0. (d)-(e): Cell density profiles predicted by the three-species heterogeneous model, $\mathcal{P}(x,t)$ (solid red), superimposed with density profiles given by the single-species homogeneous model calibrated with the best-fit value of f_0, $P(x,t)$ (solid blue). The black arrow denotes the best-fit value of interaction force, $f_0 = 0.07\,\mu$m/h. The continuum results for both models are presented at $t = 0, 12, 24, 36$, and 48 h. Black arrows denote the direction of increasing time. Results in (e) show a close-up comparison right near the leading edge, denoted by the gray shaded region in (d).

B Heterogeneity in the diffusivity, D

In this data set we explore the heterogeneity in the diffusivity, D. Here we fix values of amplitude of interaction forces, $f_0 = 0.05\,\mu$m/h, and cell size, $\delta = 34\,\mu$m. To analyse performance of the single-species homogeneous model (Equation (3.9), Main paper) applied to a data generated by the three-species heterogeneous model (Equations (3.2)-(3.4), Main paper) we consider four different diffusivity distributions: (i) uniform distribution, Figure B.1(a), (ii) monotonically decreasing distribution, Figure B.2(a), (iii) non-monotonic distribution, Figure B.3(a), and (iv) monotonically increasing distribution, Figure B.4(a). For all cases presented we are able to predict a position of the leading edge as well as accurately describe cell density profiles given by the three-species heterogeneous model.

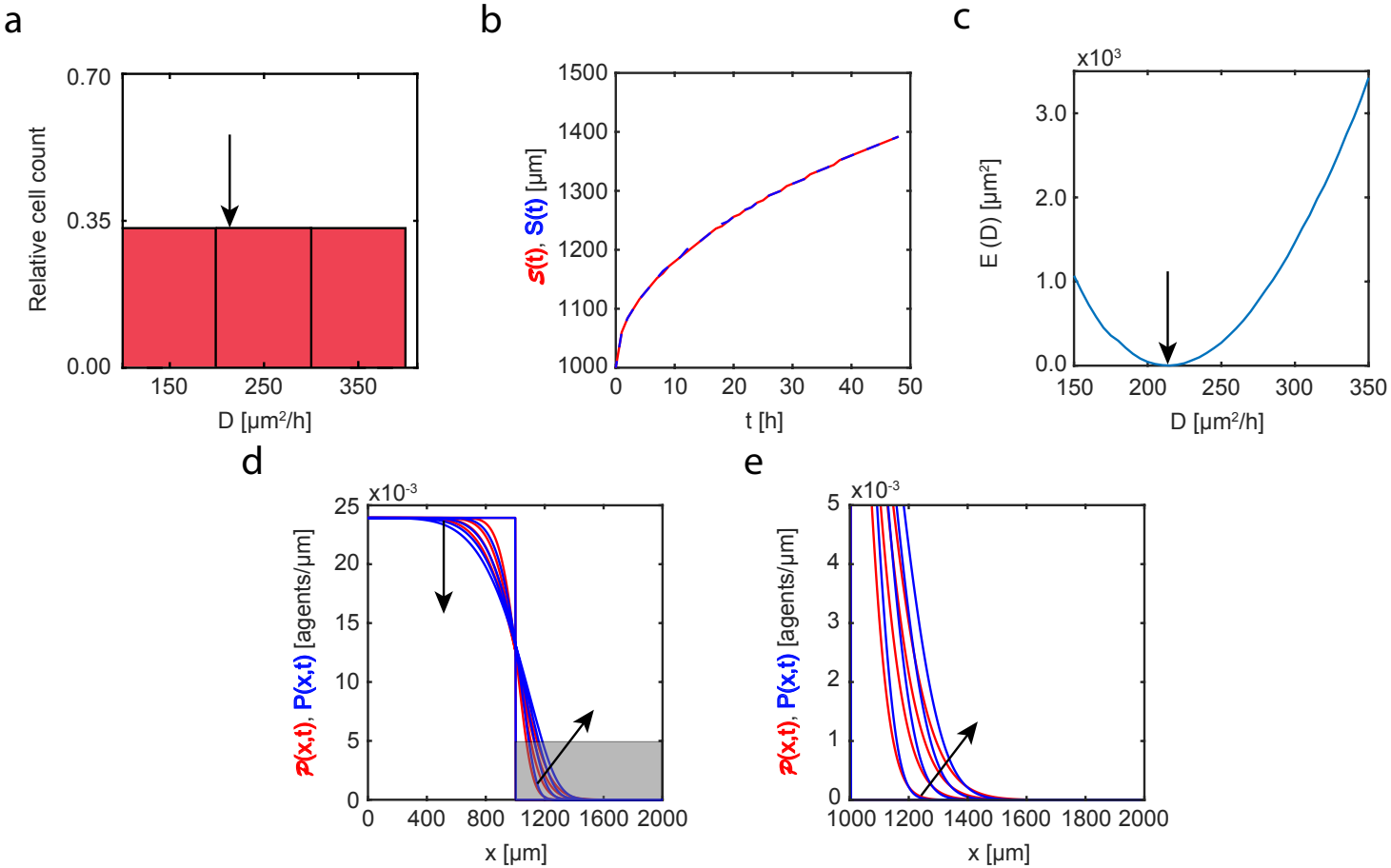

Fig. B.1. Set IIIa. Heterogeneity in diffusivity: uniform distribution. (a): Diffusivity distribution adopted in the three-species heterogeneous model, Equations (3.2)-(3.4) (Main paper). (b): Leading edge predicted by the three-species heterogeneous model, $\mathcal{S}(t)$ (solid red), and the best-fit approximation given by the single-species homogeneous model, $S(t)$ (blue dashed). (c): Error measure, $E(D)$, between the density profiles given by the three-species heterogeneous model and the profiles predicted by the single-species homogeneous model as a function of diffusivity, D. The black arrow denotes the best-fit value of diffusivity, $D = 215\,\mu\text{m}^2/\text{h}$. (d)-(e): Cell density profiles predicted by the three-species heterogeneous model, $\mathcal{P}(x,t)$ (solid red), superimposed with density profiles given by the single-species homogeneous model calibrated with the best-fit value of D, $P(x,t)$ (solid blue). The continuum results for both models are presented at $t = 0, 12, 24, 36$, and $48\,\text{h}$. Black arrows denote the direction of increasing time. Results in (e) show a close-up comparison right near the leading edge, denoted by the gray shaded region in (d).

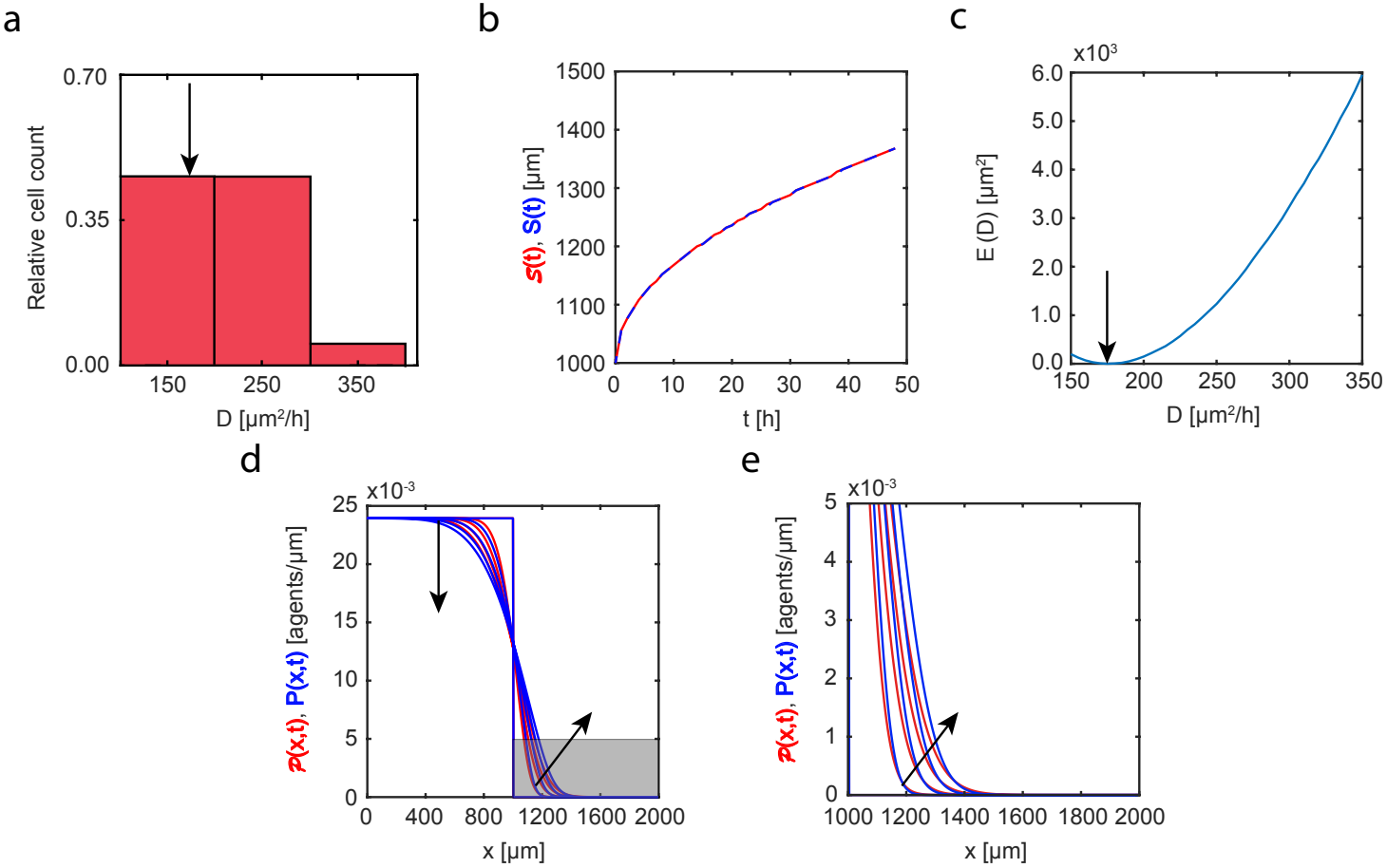

Fig. B.2. Set IIIb. Heterogeneity in diffusivity: monotonically decreasing distribution. (a): Diffusivity distribution adopted in the three-species heterogeneous model, Equations (3.2)-(3.4) (Main paper). (b): Leading edge predicted by the three-species heterogeneous model, $\mathcal{S}(t)$ (solid red), and the best-fit approximation given by the single-species homogeneous model, $S(t)$ (blue dashed). (c): Error measure, $E(D)$, between the density profiles given by the three-species heterogeneous model and the profiles predicted by the single-species homogeneous model as a function of diffusivity, D. The black arrow denotes the best-fit value of diffusivity, $D = 175\,\mu\text{m}^2/\text{h}$. (d)-(e): Cell density profiles predicted by the three-species heterogeneous model, $\mathcal{P}(x,t)$ (solid red), superimposed with density profiles given by the single-species homogeneous model calibrated with the best-fit value of D, $P(x,t)$ (solid blue). The continuum results for both models are presented at $t = 0, 12, 24, 36$, and $48\,\text{h}$. Black arrows denote the direction of increasing time. Results in (e) show a close-up comparison right near the leading edge, denoted by the gray shaded region in (d).

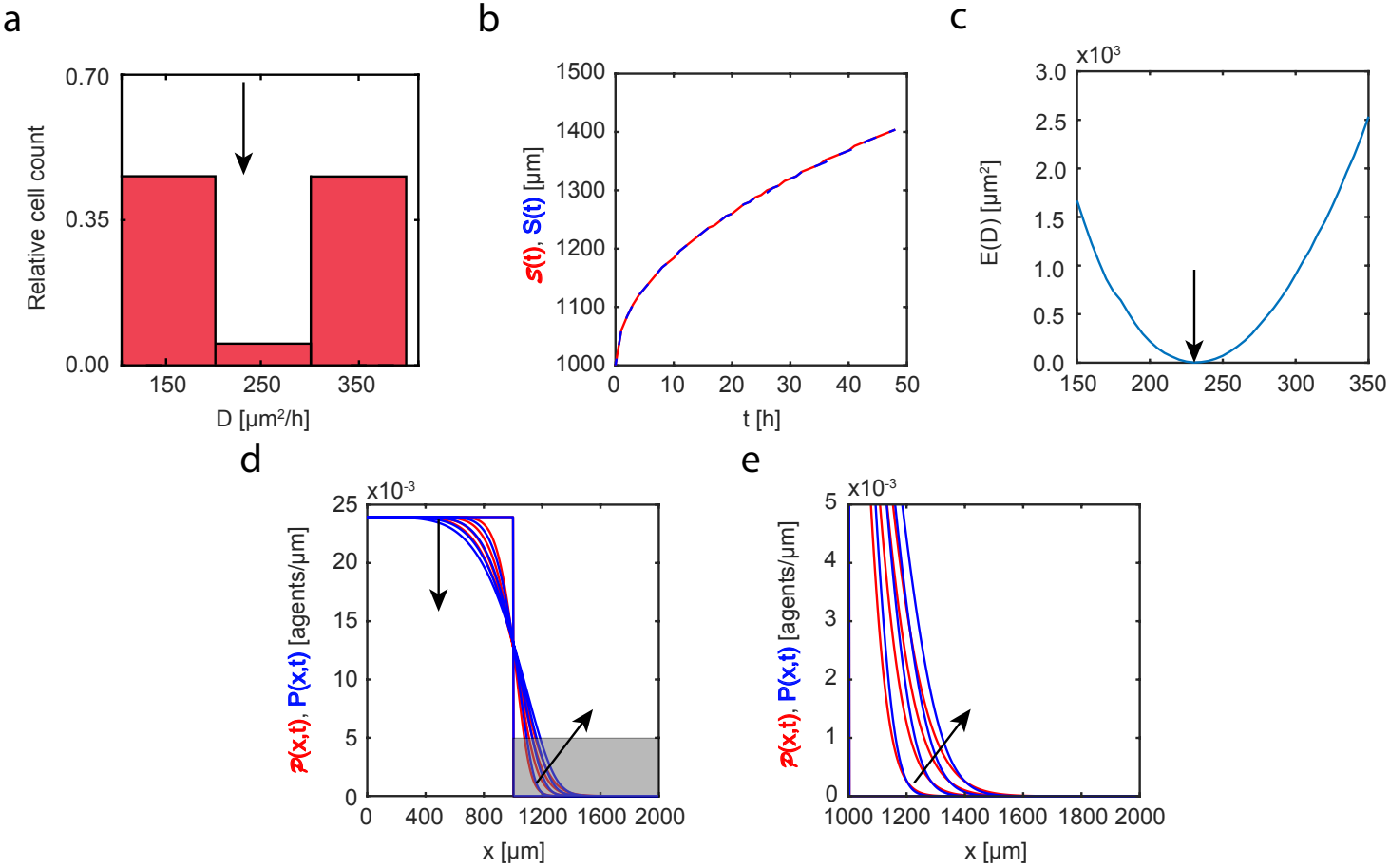

Fig. B.3. Set IIIc. Heterogeneity in diffusivity: non-monotonic distribution. (a): Diffusivity distribution adopted in the three-species heterogeneous model, Equations (3.2)-(3.4) (Main paper). (b): Leading edge predicted by the three-species heterogeneous model, $\mathcal{S}(t)$ (solid red), and the best-fit approximation given by the single-species homogeneous model, $S(t)$ (blue dashed). (c): Error measure, $E(D)$, between the density profiles given by the three-species heterogeneous model and the profiles predicted by the single-species homogeneous model as a function of diffusivity, D. The black arrow denotes the best-fit value of diffusivity, $D = 230\,\mu\text{m}^2/\text{h}$. (d)-(e): Cell density profiles predicted by the three-species heterogeneous model, $\mathcal{P}(x,t)$ (solid red), superimposed with density profiles given by the single-species homogeneous model calibrated with the best-fit value of D, $P(x,t)$ (solid blue). The continuum results for both models are presented at $t = 0, 12, 24, 36$, and $48\,\text{h}$. Black arrows denote the direction of increasing time. Results in (e) show a close-up comparison right near the leading edge, denoted by the gray shaded region in (d).

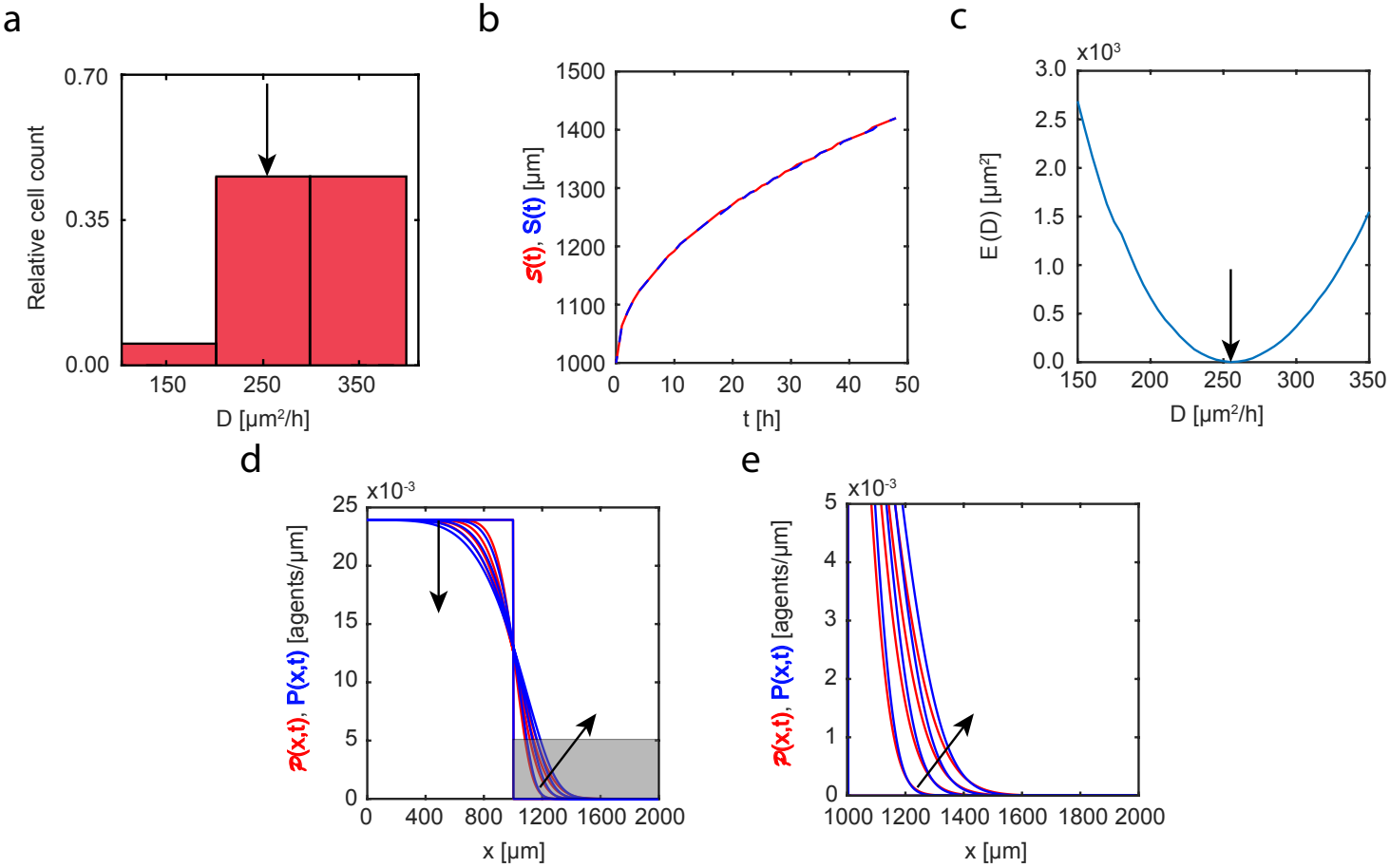

Fig. B.4. Set IIId. Heterogeneity in diffusivity: monotonically increasing distribution. (a): Diffusivity distribution adopted in the three-species heterogeneous model, Equations (3.2)-(3.4) (Main paper). (b): Leading edge as predicted by the three-species heterogeneous model, $\mathcal{S}(t)$ (solid red), and the best-fit approximation given by the single-species homogeneous model, $S(t)$ (blue dashed). (c): Error measure, $E(D)$, between the density profiles given by the three-species heterogeneous model and the profiles predicted by the single-species homogeneous model as a function of diffusivity, D. The black arrow denotes the best-fit value of diffusivity, $D = 255\,\mu\text{m}^2/\text{h}$. (d)-(e): Cell density profiles as predicted by the three-species heterogeneous model, $\mathcal{P}(x,t)$ (solid red), superimposed with density profiles given by the single-species homogeneous model calibrated with the best-fit value of D, $P(x,t)$ (solid blue). The continuum results for both models are presented at $t = 0, 12, 24, 36$, and $48\,\text{h}$. Black arrows denote the direction of increasing time. Results in (e) show a close-up comparison right near the leading edge, denoted by the gray shaded region in (d).

C Discretisation scheme for the single-species homogeneous model and heterogeneous three-species model

In this section we present the discretisation scheme used to obtain the numerical solution of the single-species homogeneous model in the mean-field framework. In summary, the governing equation that we consider is as follows,

$$\frac{\partial P(x,t)}{\partial t} = D\Delta P(x,t) - (N-1)\nabla(P(x,t)\,V(x,t)), \tag{C.1}$$

where

$$V(x,t) = \int F(x-y)\,P(y,t)\,\mathrm{d}y \tag{C.2}$$

is the velocity filed induced by intercellular interaction forces, and $N = 36$ is the total number of cells in the simulations.

To present the numerical scheme as succinctly as possible, we define

$$\sigma(x,y,t) = F(x-y)\,P(y,t), \tag{C.3}$$

$$\begin{aligned} I_s &= P(x_s,t)\int \sigma(x_s,y)\,\mathrm{d}y \\ &= P(x_s,t)\frac{h}{2}\sum_i \Big[\sigma(x_s,y_{i+1}) + \sigma(x_s,y_i)\Big] + O(h^2), \end{aligned} \tag{C.4}$$

where the rectangle rule with step h is used for numerical integration, and indices s and i denote the equally-spaced spatial mesh nodes.

Using the definitions in Equations (C.3)-(C.4), we apply the method of lines to Equation (C.1) and obtain the following system of coupled ordinary differential equations,

$$\frac{\mathrm{d}P_i}{\mathrm{d}t} = \frac{D}{h^2}\Big[P_{i+1} - 2P_i + P_{i-1}\Big] - (N-1)\frac{1}{2h}\Big[I_{i+1} - I_{i-1}\Big], \tag{C.5}$$

where index i denotes a spatial mesh node. This systems of ordinary differential equations is solved using an explicit forward Euler algorithm with constant time steps of duration Δt.

Similarly, the three-species model is given by three coupled integro-PDEs in the following form,

$$\frac{\partial p^{(1)}}{\partial t} = D_1 \Delta p^{(1)} - (n_1 - 1)\nabla(p^{(1)}\, V^{(11)}) - n_2 \nabla(p^{(1)}\, V^{(12)}) - n_3 \nabla(p^{(1)}\, V^{(13)}), \tag{C.6}$$

$$\frac{\partial p^{(2)}}{\partial t} = D_2 \Delta p^{(2)} - (n_2 - 1)\nabla(p^{(2)}\, V^{(22)}) - n_1 \nabla(p^{(2)}\, V^{(21)}) - n_3 \nabla(p^{(2)}\, V^{(23)}), \tag{C.7}$$

$$\frac{\partial p^{(3)}}{\partial t} = D_3 \Delta p^{(3)} - (n_3 - 1)\nabla(p^{(3)}\, V^{(33)}) - n_1 \nabla(p^{(3)}\, V^{(31)}) - n_2 \nabla(p^{(3)}\, V^{(32)}), \tag{C.8}$$

$$V^{(lk)} = \int_\Omega F^{(lk)}(x - y)\, p^{(k)}(y, t)\, \mathrm{d}y. \tag{C.9}$$

We define

$$\sigma^{lk}(x, y, t) = F^{(lk)}(x - y)\, p^{(k)}(y, t), \tag{C.10}$$

$$\begin{aligned} I_s^{lk} &= p^{(l)}(x_s, t) \int \sigma^{lk}(x_s, y)\, \mathrm{d}y \\ &= p^{(l)}(x_s, t) \frac{h}{2} \sum_i \Big[\sigma^{lk}(x_s, y_{i+1}) + \sigma^{lk}(x_s, y_i)\Big] + O(h^2), \end{aligned} \tag{C.11}$$

where $k = 1, 2, 3$ is the subpopulation index, indices i and s denote the equally-spaced spatial mesh nodes, and h is spatial discretisation step.

Using the definitions in Equations (C.10)-(C.11), we apply the method of lines to Equations (C.6)-(C.8) and obtain the following system of coupled ordinary differential equations,

$$\frac{\mathrm{d}p_i^{(k)}}{\mathrm{d}t} = \frac{D_k}{h^2}\Big[P_{i+1}^{(k)} - 2P_i^{(k)} + P_{i-1}^{(k)}\Big] - (n_k - 1)\frac{1}{2h}\Big[I_{i+1}^{kk} - I_{i-1}^{kk}\Big] - \sum_{l \neq k} n_l \frac{1}{2h}\Big[I_{i+1}^{lk} - I_{i-1}^{lk}\Big], \tag{C.12}$$

where $k = 1, 2, 3$ is the subpopulation index.